2003

Application of mechanistic models in predicting flow behavior in deviated wells under UBD conditions

Faisal Abdullah ALAdwani
Louisiana State University and Agricultural and Mechanical College, faladw1@lsu.edu

APPLICATION OF MECHANISTIC MODELS IN PREDICTING FLOW BEHAVIOR IN DEVIATED WELLS UNDER UBD CONDITIONS

A Thesis

Submitted to the Graduate Faculty of the
Louisiana State University and
Agricultural and Mechanical College
in partial fulfillment of the
Requirements for the degree of
Master of Science in Petroleum Engineering
in
The Department of Petroleum Engineering

by
Faisal Abdullah ALAdwani
B.Sc., Kuwait University, 1998
May, 2003

Acknowledgements

At this opportunity the author would like to express great appreciation to Dr. Jeremy K. Edwards for supervising this work and his valuable guidance and genuine interest in completing this study. The author is greatly indebted to his country, Kuwait, for supporting his education through the scholarship from Kuwait University. Also special thanks extend to the other members of the committee, Dr. Julius Langlinais and Dr. John Smith for their valuable advice and suggestions. In addition, a special thanks extends to Mr. Adel AL-Khayat from KUFPEC on his advice on field operations. Finally, the author is grateful to the LSU Craft & Hawkins department of petroleum engineering for giving the opportunity to complete this study under their supervision.

Table of Contents

List of Tables

List of Figures

Abstract

Underbalanced drilling (UBD) has increased in recent years because of the many advantages associated with it. These include increase in the rate of penetration and reduction of lost circulation and formation damage. Drilling of deviated and horizontal wells also increased since recovery can be improved from a horizontal or a deviated well. The drilling of deviated wells using UBD method will reduce several drilling related problems such as hole cleaning and formation damage. Prediction of flow and pressure profiles while drilling underbalanced in such wells will help in designing and planning of the well. The main aim of this research is to study and model the effect of well deviation on pressure and flow profile in the drillstring and the annulus under UBD conditions through the use of mechanistic two phase flow models. Specifically, a current model is modified to include effects of wellbore deviation. Simulation results are compared with data from a deviated well drilled with UBD technology.

Chapter 1

Introduction

Underbalanced drilling is the drilling process where the effective bottomhole circulation pressure of the fluid system is less than the formation pressure. UBD can be achieved by injecting lightened drilling fluid such as gas, mist, foam, and diesel, which will create such low pressure in order not to overcome the formation pressure.

The main reasons to perform UBD operations are listed below[1].

- Increased bit life and rate of penetration.
- Minimize lost circulation and differential sticking.
- Reduce formation damage and stimulation requirements.
- Environmental benefits.

Performing UBD operations on deviated or horizontal wells requires controlling the drilling parameters in order not to damage the formation and to achieve the maximum rate of penetration. In order to optimize the use of UBD in any well, a successful control of the bottomhole pressure and fluid flowing through the formation is necessary.

Some of the damage mechanisms that may occur in both horizontal and vertical wells are listed below[2]:

- Rock and fluid flow incompatibilities.
- Solid invasion.
- Chemical adsorption/wettability.
- Fines migration.
- Biological activities.

In addition, some of the damages that occurs during UBD operations may include:

- Lack of protective sealing filter cake.
- Spontaneous countercurrent imbibition effects, which allow the entrainment of potentially damaging fluid filtrate into the reservoir matrix in the near wellbore region.
- Glazing and surface damage effects caused by insufficient heat conductivity capacity of circulating fluids.

During UBD operations, a complex fluid system occurs both inside the drillstring and the annulus. Two phase flow prediction techniques are used to predict several parameters such as pressure drops (both inside the drillstring and through the annulus), flow patterns, velocities, liquid holdup, and other parameters. In order to achieve this task, a set of mechanistic two phase flow models are used. It has been shown in the literature that mechanistic models accurately predict the flow pattern and liquid holdup. These models are based on the physical phenomena of the complex fluid system and flow rather than the use of empirical correlations, which are based mainly on experimental data.

Chapter 2

Literature Review

Several techniques are used in order to achieve the optimum result while performing UBD operations. The main approach used to predict the flow behavior of wells under UBD conditions is the use of the two phase flow concepts. Currently available computer models use different approaches for predicting the behavior under such conditions. Three main approaches are used in the development of such computer models, as follows :

- Homogenous approach.
- Empirical correlations approach.
- Mechanistic approach.

The homogenous approach was first used by Guo et al[3]. Their model calculated the required air rate for both maximum rate of penetration and cutting transport in foam drilling operations. They assumed that the foam can be treated as a two phase fluid in the bubbly region despite the fact that they recognized the main flow patterns (bubble, slug, churn, and annular).

The empirical correlations are formulated by establishing a mathematical relation based on experiments. Application of empirical models is limited to the data range used to generate the model. Liu et al[4] developed a computer algorithm which analyzed the behavior of foam in UBD operation, considering it as a two phase mixture. They calculated the frictional pressure drop using the mechanical energy equation coupled with a foam rheology model using an equation of state. In addition, they united their model with the Beggs and Brill[5] method for calculating bottomhole pressure and developed a computer program called MUDLITE[6,7]. The current version of MUDLITE includes other two phase flow correlations in addition to Beggs and Brill such as Orkiszewski, Hagedorn-Brown, and others. Despite the fact that the used correlation

gives good results under certain flow conditions (such as stable flow in an oil well) none of the previous models were developed for actual field conditions. Tian[8,9] developed a commercial computer program named Hydraulic UnderBalanced Simulator (HUBS), which was used in assisting engineers to design UBD operations especially for the process of optimizing circulation rate and obtaining sufficient hole cleaning. HUBS uses empirical correlations for the UBD hydraulic calculations in addition to the developed mathematical model.

Mechanistic models were developed significantly in recent years. Those models are based on a phenomenological approach that takes into account basic principles (conservation of mass and energy). Bijleveld et al.[10] developed the first steady state computer program using mechanistic approach where bottomhole pressure and two phase flow parameters were calculated by using a trial and error procedure. Stratified flow was initially assumed and then checked for validity. If the guessed flow pattern does not exist, another flow pattern is assumed and the same procedure is repeated. An average absolute error of 10% was reported compared with an average absolute error of 12% shown by Beggs and Brill. Several authors developed mechanistic models to predict accurately different flow parameters such as flow pattern, film thickness, rise velocity of gas bubbles in liquid columns, and liquid holdup. Ansari et al.[11] presented his model for upward vertical two phase flow in pipes. They did not include any effect of inclination although it exists in the model. Gomez, et al.[12] develped a unified mechanistic model for predicting the flow parameters while Kaya et al.[13] developed a comprehensive mechanistic model for predicting the flow parameters in deviated wells. Caetano et al.[14,15] developed a model for upward vertical flow in the annulus. Hasan and Kabir[16] developed a model for predicting two phase flow in annuli where they estimated the gas void fraction in during upward simultaneous two phase flow by using the drift flux approach between the liquid slug and the Taylor bubble. Lage et al.[17] developed a mechanistic model for predicting upward two phase flow in concentric

annulus. Recently, Perez-Tellez et al.[18] developed an improved, comprehensive mechanistic steady state model for pressure prediction through a wellbore during UBD operations in vertical wells; the model was validated against an actual well and full-scale well data, where it shows good performance (absolute average error less than 5%).

Gavignet and Sobey[19] reported that the drill pipe eccentricity has a large effect on the bed thickness. They reported that once the interfacial area decreases with increasing in the thickness of the cutting bed in deviated well. Hence in order to maintain an adequate movement of the mud in the annulus a large increase in the velocity is required to maintain interfacial friction carrying the cuttings up the annulus. In a deviated well, the pipe is most likely to be in an eccentric geometry in certain location. In addition Brown and Bern[20] stated that the extremes positions that reflect a realistic downhole position of drillpipe is an eccentricity of 75% which most likely occurs by a tool joint touching the bottom of the hole in a drillpipe centralized in the casing at limiting position.

Chapter 3

Model Development

The key factor for a successful UBD operation is to achieve the objectives for switching to UBD as discussed in Chapter 1. In order to achieve such success, the bottomhole pressure should be maintained within a pressure window that is bounded by below by the formation pore pressure and above by the wellbore stability pressure or surface facilities restrictions. Hence, the prediction of wellbore pressure should be as accurate as possible in order to assist in designing equipment needed to switch to UBD operations. In the past, the key approach used to predict wellbore pressure has been to use empirical multiphase flow correlations. As discussed in Chapter 2, those techniques often do not accurately match the field cases in which we are interested. In addition, those correlations are typically valid only for the range of conditions used to create the correlation.

Recently, development of mechanistic models has allowed accurate prediction of wellbore pressure. Many UBD operations require the use of nitrified diesel as the drilling fluid. Thus two phase flow will exist both in the drill pipe and the annulus. In addition, the procedure used to apply those mechanistic models in order to accurately predict wellbore pressure will be discussed, along with the major assumptions used in the model development.

3.1 Model Assumptions

In most UBD operation the drilling fluid (gasified liquid) is injected in the drillstring down through the bit and then up the annulus, where it will mix with formation rock cuttings and produced fluids form the formation.

The following assumptions were needed in order to model the behavior of a UBD operation as a two phase flow system in which only gas and liquid exists.

- The injection and formation fluids (liquid and gas) will flow at the same velocity.
- Mixture velocity and viscosity will be used instead of the usual mud cleaning rheology models because of the turbulent hole cleaning produced by the high friction gradients which results from multiphase flow of the mixture of injected and produced fluids.
- Effects of cutting transport are neglected.

3.2 Multiphase Flow Concepts

During the simultaneous flow of gas and liquid, the most distinguished aspect of such flow is the inconsistency of the distribution of both phases in the wellbore. The term flow pattern is used to distinguish such distribution, which depends on the relative magnitude of forces acting on the fluids[21]. The following terms are defined in order to assist in the multiphase flow calculations.

3.2.1 Liquid Holdup

Liquid holdup (H_L) is defined as the fraction of a pipe cross-section or volume increment that is occupied by the liquid phase[22]. The value of H_L ranges from 0 (total gas) to 1 (total liquid). The liquid holdup is defined by

$$H_L = \frac{A_L}{A_P} \tag{3.1}$$

where A_L is the pipe area of the liquid occupied by the liquid phase and A_P is pipe cross-sectional area.

The term void fraction or gas holdup is defined as the volume fraction occupied by the gas where

$$\alpha = 1 - H_L \tag{3.2}$$

When the two fluids travel at different velocities then the flow is referred to as a slip flow. No slip flow occurs when the two fluids travels at the same velocity. Hence, the term no slip liquid holdup can be defined as the ratio of the volume of liquid in a pipe element that would exist if the gas and liquid traveled at the same velocity divided by the volume of the pipe element[22]. The no-slip holdup (λ_L) is defined as follows:

$$\lambda_L = \frac{q_L}{q_L + q_G} \tag{3.3}$$

where q_L is the in-situ liquid flow rate and q_G is the in-situ gas flow rate.

3.2.2 Superficial Velocity

Superficial velocity is the velocity that a phase would travel at if it flowed through the total cross sectional area available for flow[22]. Thus, the liquid and gas superficial velocities are defined by :

$$v_{SL} = \frac{q_L}{A_P} \tag{3.4}$$

and

$$v_{SG} = \frac{q_G}{A_P} \tag{3.5}$$

The mixture velocity can be defined as the velocity of the two phases together, as follow :

$$v_M = \frac{q_L + q_G}{A_P} = v_{SL} + v_{SG} \tag{3.6}$$

The in-situ velocity is the actual velocity of the phase when the two phases travel together. They can be defined as follows :

$$v_L = \frac{v_{SL}}{H_L} \tag{3.7}$$

and

$$v_G = \frac{v_{SG}}{H_G} = \frac{v_{SG}}{1 - H_L} \tag{3.8}$$

When water exists in addition to the liquid and gas, a weighting factor is introduced to take care of the slippage that could occur between different liquid phases that exists during drilling (drilling fluid, produced oil and produced water). This factor is defined as follows:

$$f_o = \frac{q_{DF}}{q_{DF} + q_O + q_w} \tag{3.9}$$

where q_{DF} is the drilling fluid flow rate, q_O inflow oil flow rate, and q_w is inflow water flow rate.

3.2.3 Fluid properties

Mixture fluid properties (density and viscosity) can be calculated for the case of no-slip or slip flow. Mixture density and viscosity are calculated using a weighted average technique based on the in-situ liquid holdup.

3.2.4 Two Phase Flow Patterns

As mentioned above, the variation in the physical distribution of the phases in the flow medium creates several flow patterns. Multiphase flow patterns highly depend on flow rates, wellbore geometry, and the fluid properties of the phases. In addition, flow patterns can change with variation in wellbore pressure and temperature. The major flow patterns that exist in multiphase flow are dispersed bubble, bubble, slug, churn and annular. Figure 3.1 shows different flow patterns exists in a pipe.

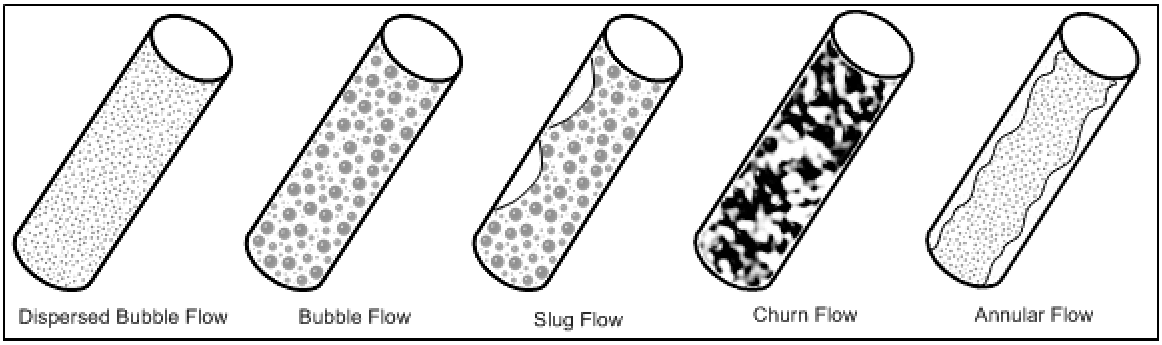

Figure 3.1: Different Flow Patterns in Two Phase Flow.

- **Dispersed Bubble Flow:** This flow is characterized by gas being distributed in small spherically shaped bubbles in a continuous liquid phase. Dispersed bubble occurs at low gas flow rates and high liquid rates. In dispersed bubble flow, both phases flow at nearly the same velocity. No slip is seen between the phases and the flow is essentially homogenous.
- **Bubble flow:** This flow characterized by a discontinuous gas phase, which is distributed as discrete bubbles inside a continuous liquid phase. The discrete gas bubbles tend to slightly deviate from spherical shape and exhibit slippage through the liquid phase due to buoyancy forces. This pattern occurs at low to medium superficial velocities.
- **Slug Flow:** This flow is characterized by a series of slug units. Each unit is composed of alternating gas pockets and plugs of liquid called slugs. In vertical flow the gas pocket is commonly referred to as a Taylor Bubble. A film of liquid exists around the pocket flowing downward relative to the gas bubble. The liquid slug, carrying distributed small gas bubbles, bridges the conduit and separates two consecutive gas bubbles.
- **Churn Flow:** This flow pattern exists in upward flow only and is very chaotic in nature. The shape of the Taylor bubble and the liquid slug are irregular and seemingly random. Churn flow can be considered to be a transition between bubbly flow and fully developed slug flow.

- **Annular Flow:** This flow pattern is characterized by the axial continuity of gas phase in a central core with the liquid flowing upward, both as a thin film along the pipe wall and as a dispersed droplets in the core. A small amount of liquid is entrained in the light velocity core region. Annular flow occurs at high gas superficial velocities with relatively little liquid present.

Transition boundaries between the various flow patterns can be plotted on a flow pattern map. Flow pattern maps have been determined experimentally from a wide range of conditions. Taitel et al[23] has studied and identified those flow patterns in pipes. Figure 3.2 shows a typical flow pattern map for downward vertical two phase flow where Figure as developed by Taitel et al.[23]. Figure 3.3 shows the flow pattern map used in the annulus which was developed by Caetano et al.[14,15]. Both figures below are made for certain flow geometries and fluid properties.

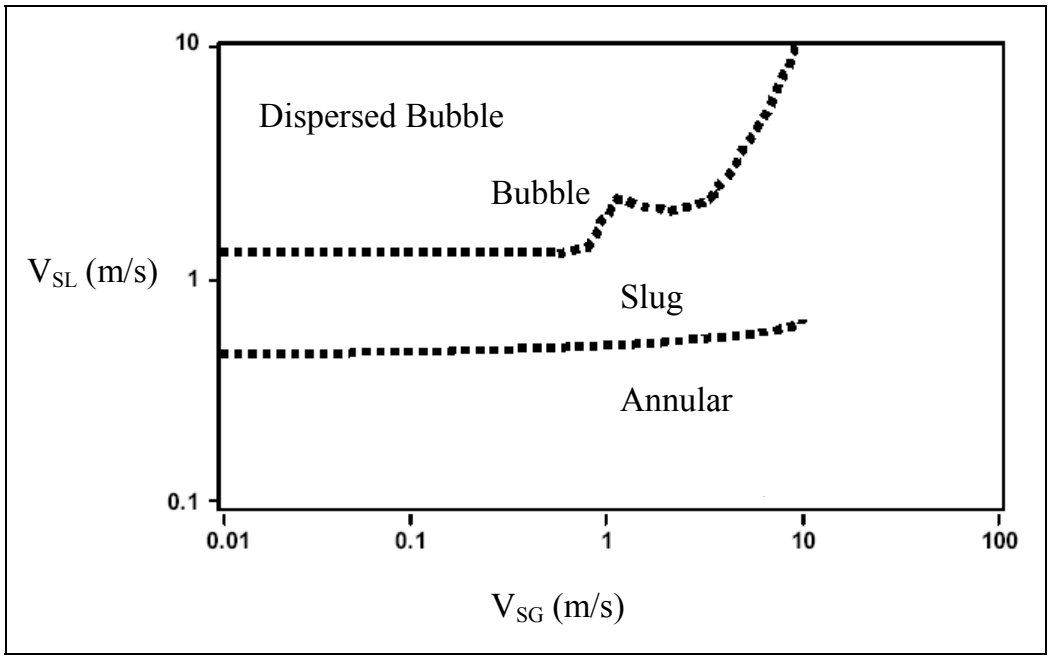

Figure 3.2: Flow Pattern Map for Downward Two Phase Flow in Pipes (After Taitel et al.[23])

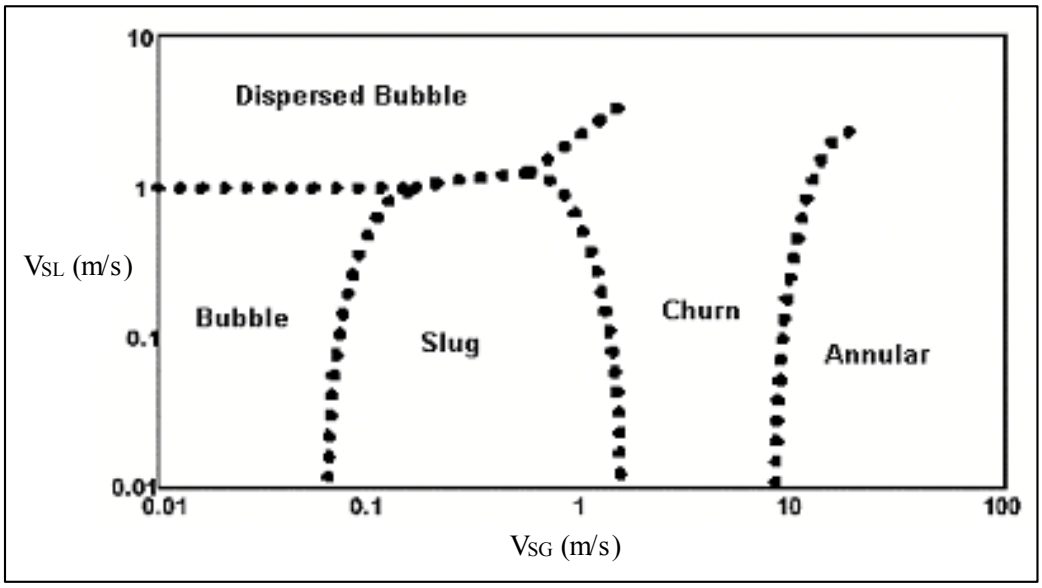

Figure 3.3: Flow Pattern Map for Upward Two Phase Flow in Annulus (After Caetano et al[14,15])

3.2.5 UBD Flow Patterns

In a typical UBD operation and based on liquid and gas injection rates, certain flow patterns exists either in the drillstring or in the annulus. Perez-Tellez et al.[18] shows that in the annulus very high superficial velocities would be observed when the flow is at atmospheric pressure. Also any small increase in the choke pressure would be enough to significantly decrease those superficial velocities and thus shift the flow pattern from annular to either slug or churn. This phenomenon is shown graphically in Figure 3.4, where it shows typical superficial velocities for typical injection gas and flow rates for UBD conditions[18]. Those velocities reflect the actual conditions near the surface in terms of flow patter in a typical UBD operation.

As can be seen in Figure 3.4 for the upward flow in the annulus, churn flow may occur near the top of the well. For downward flow through the drillstring slug, bubble, and dispersed bubble may occur, depending on the combination of injected gas and liquid flow rates. Those flow pattern are the most commonly seen in a typical UBD operations. In the following section detailed calculations of those flow patterns are shown.

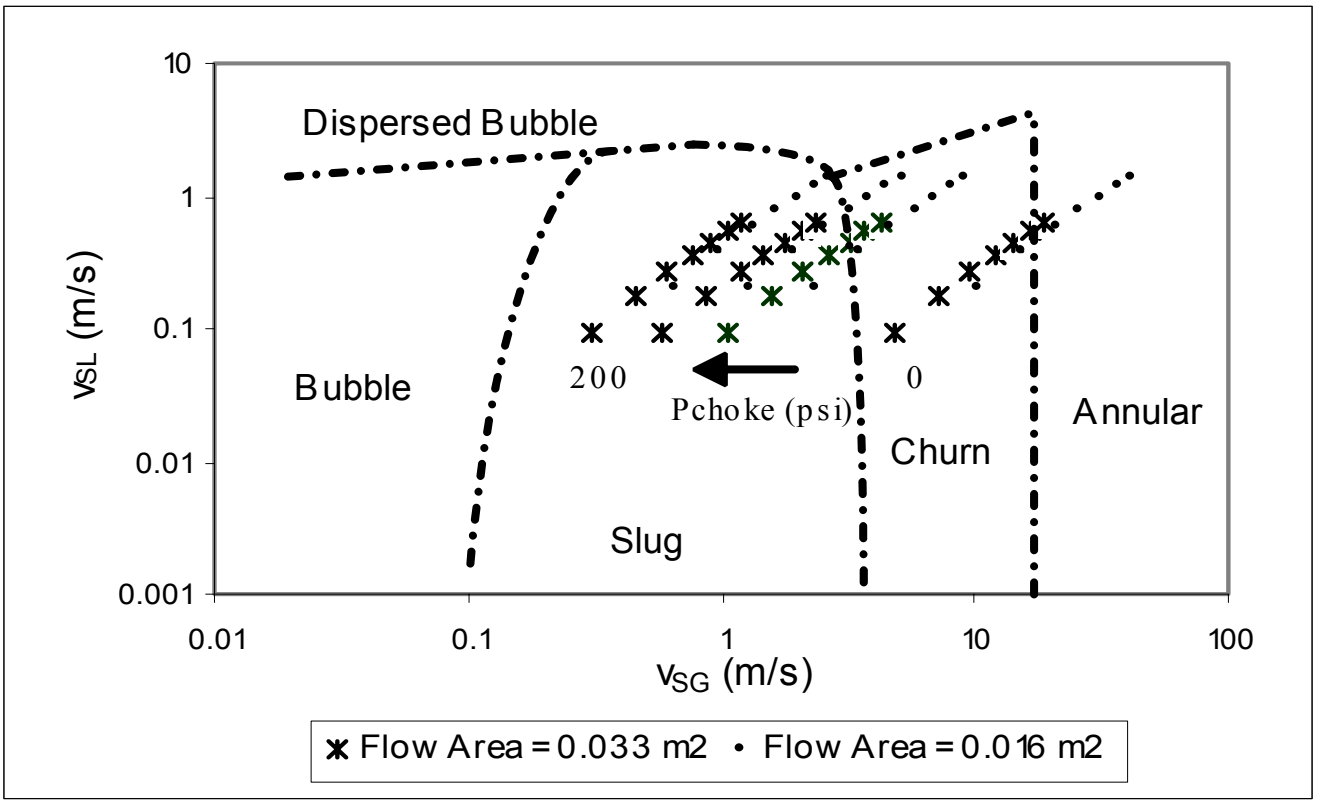

Figure 3.4: Near Surface Annular Flow Pattern in UBD Operations (After Perez-Tellez et al.[18])

3.3 Flow Pattern Prediction Models

The following flow pattern models applied to both the drillstring and the annulus with an inclination angle θ from horizontal.

3.3.1 Downward Flow through the Drillstring

- **Bubble to Slug Transition**

Hasan[24] stated that the transition from bubbly to slug flow occurs because of the bubble agglomeration resulting from increased collision between bubbles at higher void fraction. In addition, Hasan[24] stated that the same void fraction used for upward flow could be used for the case of downward flow. Hasan[24] observed that this transition occurred at a void fraction of 0.25. Also, the rise velocity is unaffected by pipe inclination angle and in deviated wells, the bubbles

prefer to flow near the upper wall of the pipe, causing a higher local void fraction compared with the cross-sectional average value[24]. Hasan[25] and Hasan and Kabir[26] derived an equation for bubble to slug transition flow for upward flow in deviated wells. Hasan[24] proposes the same equation for a downward flow using a negative terminal rise velocity. Hasan[24] proposed the following expression for transition boundary between bubble and slug flow:

$$v_{SG} = \frac{C_O v_{SL} - v_\infty}{(1/\alpha) - C_O} \sin\theta \qquad 3.10$$

Harmathy[27] correlation is used to calculate the terminal rise velocity (v_∞) for upward flow in vertical and inclined channels as follows:

$$v_\infty = 1.53\left[\frac{(\rho_L - \rho_G)g\sigma}{\rho_L^2}\right]^{0.25} \qquad 3.11$$

The velocity profile coefficient (C_O) has been defined by Zuber and Findlay[28] due to the effect of non-uniform flow and concentration distribution across the pipe and the effect of local relative velocity between the two phases. Table 3.1 shows the values for the velocity profile coefficients for different inclination angles as given by Alves[29]

Table 3.1: Flow Coefficients for Different Inclination Angle Ranges (After Alves[29])

Inclination Angle (Degrees)	Co
10-50	1.05
50-60	1.15
60-90	1.25

In addition, Wallis[30] has proposed that the effect of single bubble rising in a swarm of bubbles can be introduced by defining a bubble swarm effect (n), thus H_L^n will be taken into

consideration. Finally, Perez-Tellez et al[18] proposed the use of the combined effect of the bubble swarm effect (n) and the velocity profile coefficient (C_O) and introduced the following expression for the bubble slug transition

$$v_G - C_o v_m = v_\infty H_L^n \tag{3.12}$$

Applying Equation 3.12 to Hasan approach in order to find the criteria from bubble to slug yields the following equation

$$v_{SL} = \frac{(1/\alpha - C_O)v_{SG}/\sin(\theta) + v_\infty H_L^n}{C_O} \tag{3.13}$$

with a gas void fraction $\alpha = 0.25$.

- **Bubble or Slug to Dispersed Bubble Transition**

Hasan and Kabir[16] find that the model which was created by Taitel et al[23] was applicable for flow through vertical and inclined annuli. Based on the maximum bubble diameter possible under highly turbulent conditions the model following model could be used to find the relation ship between phase velocities, pipe diameters, and fluid properties[24]. Perez-Tellez[31] recommended the use of the equation developed by Caetano[14,15] as shown below where ID is the inner pipe diameter.

$$v_M^{1.2}\left(\frac{2f_F^{0.4}}{ID}\right)^{0.4}\left[\frac{1.6\sigma}{(\rho_L-\rho_G)g}\right]^{0.5}\left(\frac{\rho_L}{\sigma}\right)^{0.6} = 0.725 + 4.15\left(\frac{v_{SG}}{v_M}\right)^{0.5} \tag{3.14}$$

Equation 3.14 shows that in order to calculate the homogenous fanning friction factor, and since the rise velocity for the dispersed bubble flow is very small compared to the local velocities, the no-slip holdup (λ_L) could be used to calculate f_F.

3.3.2 Upward Flow through the Annuli

Several authors[14,15,16,17] agreed on using the method proposed by Taitel et al[23] for predicting flow pattern, in addition to his model and coupling it with the bubble swarm effect and the velocity swarm coefficient. The flow patterns used were shown in Figure 3.3 where the transition boundaries will be calculated based on different flow geometry and properties.

- **Bubble to Slug Transition**

During bubble flow, discrete bubbles rise with the occasional appearance of a Taylor bubble. The discrete bubble rise velocity was defined in Equation 3.11. Hasan and Kabir[16] stated that the presence of an inner tube tends to make the nose of the Taylor bubble sharper, causing an increase in the Taylor bubble rise velocity. As a result, Hasan and Kabir[15] developed Equation 3.15 where the diameter of the outer tube should be used with the diameter ratio (OD/ID) to get the following expression for the Taylor bubble rise velocity in inclined annulus

$$v_{TB} = (0.345 + 0.1*(OD/ID))\sqrt{\sin\theta}(1+\cos\theta)^{1.2}\sqrt{gID\frac{\rho_L - \rho_G}{\rho_L}} \qquad 3.15$$

where

OD : Outside pipe diameter

ID : Inner casing diameter

g : Gravity acceleration

ρ_L: Liquid density

ρ_G: Gas density

Hasan and Kabir[16] stated that the presence of an inner tube does not appear to influence the bubble concentration profile (C_O) and thus the following expression could be used :

$$v_{SL} = \frac{(4 - C_O)v_{SG}}{\sin\theta} - v_{\infty} \qquad 3.16$$

- **Bubble or Slug to dispersed bubble transition**

Equation 3.14 is used to define the transition from bubble or slug to dispersed bubble flow. The hydraulic diameter (D_h) is substituted for the pipe inside diameter (ID). The hydraulic diameter of the casing-tubing annulus is given by

$$D_h = ID - OD \qquad 3.17$$

where ID is the internal casing diameter and OD is the outside pipe diameter.

- **Dispersed bubble to slug flow transition**

Taitel et al.[23] determined that the maximum allowable gas void fraction under bubble flow condition is 0.52. Higher values will convert the flow to slug, hence the transition boundary could be equated as follows :

$$v_{SL} = 0.923 v_{SG} \qquad 3.18$$

- **Slug to churn transition**

Tengesdal et al.[32] has developed a transition from slug to churn flow in an annulus. They stated that the slug structure will be completely destroyed and churn flow will occur if the gas void fraction equals 0.78. Thus churn flow will occur. The transition from slug flow to churn flow can thus be represented by :

$$v_{SL} = 0.0684 v_{sg} - 0.292\sqrt{gD_{ep}} \qquad 3.19$$

where D_{ep} is the equi-periphery diameter defined as follow

$$D_{ep} = ID + OD \qquad 3.20$$

where ID is the inner casing diameter and OD is the outer pipe diameter.

- **Churn to annular transition**

Taitel et al.[23] proposed the following transition which was supported by Hasan and Kabir[16] :

$$v_{SG} = 3.1\left[\frac{(\rho_L - \rho_G)g\sigma}{\rho_G^2}\right]^{0.25} \qquad 3.21$$

3.4 Flow Behavior Prediction Models

After determining the required flow pattern, which either exists in the drillstring or annulus, then the following behavior prediction models are applied in order to calculate the pressure gradient and phases fractions. The total pressure gradient is calculated as follows :

$$\left(\frac{dP}{dL}\right)_{total} = \left(\frac{dP}{dL}\right)_{el} + \left(\frac{dP}{dL}\right)_{f} + \left(\frac{dP}{dL}\right)_{acc} \qquad 3.22$$

Where the following are the component of the total pressure gradient

$\left(\frac{dP}{dL}\right)_{el}$ is the elevation change component

$\left(\frac{dP}{dL}\right)_{f}$ is the friction component

$\left(\frac{dP}{dL}\right)_{acc}$ is the acceleration component

3.4.1 Downward Flow through the Drillstring

- **Bubble Flow Model for Drillstring**

The drift flux approach is used to calculate liquid holdup considering the slippage between the phases and non-homogenous distribution of bubbles. Kaya et al.[13] developed an expression for the slip velocity considering inclination and bubble swarm effect. Assuming turbulent velocity profile for the mixture with rising bubbles concentrated more at the center than along the pipe wall, the slip velocity using the drift flux approach can be expressed as follows:

$$v_S = \frac{v_{SG}}{1 - H_L} - C_O v_M \qquad 3.23$$

With an inclination angle θ the proposed model[13] as shown below

$$v_S = v_\infty \sqrt{H_L \sin\theta} \qquad 3.24$$

Combining equations 3.23 and 3.24 we get the following expression

$$v_\infty \sqrt{H_L \sin\theta} = \frac{v_{SG}}{1 - H_L} - 1.2 v_M \qquad 3.25$$

Liquid holdup can be calculated from Equation 3.25 using a trial and error procedure as follow

1. Assume an initial holdup value (H_{L0}); a good guess is the no-slip holdup.
2. Calculate the holdup Equation 3.25 as follows :

$$H_L = 1 - \frac{v_{SG}}{v_\infty \sqrt{H_L \sin\theta} + 1.2 v_M} \qquad 3.26$$

3. Check the calculated value with the guessed one. If the two values of H_L agree within an acceptable tolerance then stop. Otherwise, repeat steps 1-3 until H_L converges.

After determining the holdup, mixture properties can be calculated using the following equations

$$\rho_M = \rho_L H_L + \rho_G (1 - H_L) \quad 3.27$$

$$\mu_M = \mu_L H_L + \mu_G (1 - H_L) \quad 3.28$$

The elevation pressure gradient is given by

$$\left(\frac{dP}{dL}\right)_{el} = \rho_M g \sin\theta \quad 3.29$$

The frictional pressure loss is given by

$$\left(\frac{dP}{dL}\right)_{f} = \frac{f_M \rho_M v_M^2}{2ID} \quad 3.30$$

where ID is the inner pipe diameter and f_M is the Moody friction factor and is calculated using the following Reynolds number

$$N_{RE,M} = \frac{\rho_M v_M ID}{\mu_M} \quad 3.31$$

Moody friction factor is four times the Fanning friction factor and it is calculated using the Colebrook[33] function and solving using a trial and error procedure using the Equation 3.32 :

$$\frac{1}{\sqrt{f_m}} = -4\log\left(\frac{0.269\varepsilon}{ID} + \frac{1.255}{N_{RE}\sqrt{f_m}}\right) \quad 3.32$$

where

ID: inner pipe diameter

N_{RE}: Reynolds number and

ε: pipe roughness.

The acceleration pressure gradient components is calculated using Beggs and Brill[5] approach as follow

$$\left(\frac{dP}{dL}\right)_{acc} = \frac{\rho_M v_M v_{SG}}{p}\frac{dP}{dL} \tag{3.33}$$

the acceleration term (E_k) is defined as follow

$$E_k = \frac{\rho_M v_M v_{SG}}{p} \tag{3.34}$$

Then the total pressure drop is calculated by Equation 3.35 :

$$\left(\frac{dP}{dL}\right)_{total} = \frac{\left(\frac{dP}{dL}\right)_{el} - \left(\frac{dP}{dL}\right)_{f}}{1 - E_k} \tag{3.35}$$

- **Dispersed bubble flow model for drillstring**

Since nearly a uniform bubble distribution in the liquid, the flow can be treated as a homogenous flow. Thus, the liquid holdup is very close to the no-slip holdup (λ_L). Hence, the total pressure drop is calculated using Equations 3.27-3.35.

- **Slug flow model for drillstring**

From the bubbly flow model shown above, liquid holdup for the rise velocity of a Taylor bubble in downward flow may be calculated by

$$H_{L_{TB}} = 1 - \frac{v_{SG}}{\left(C_1 v_m - v_{TB}\right)} \tag{3.36}$$

Hasan[24] recommended to use a value of C_1=1.12. The liquid holdup is calculated by Equation 3.37 :

$$H_{L_{SU}} = 1 - \left[\frac{L_{TB}}{L_{SU}}\left(1 - H_{L_{TB}}\right) + \frac{L_{LS}}{L_{SU}}\left(1 - H_{L_{LS}}\right)\right] \tag{3.37}$$

The slug unit length can be calculated by the following expression based on the superficial gas velocity

$$L_{SU} = \frac{160(ID)v_{SG}}{C_0 v_m - v_\infty} \text{ for } v_{SG} > 0.4\, m/\text{sec} \qquad 3.38$$

$$L_{SU} = \frac{64ID}{C_0 v_m - v_\infty} \text{ for } v_{SG} \le 0.4\, m/\text{sec} \qquad 3.39$$

Perez-Tellez[31] showed that, for a fully developed Taylor bubble, the total hydrostatic and frictional pressure losses can be calculated by

$$\left(\frac{dP}{dL}\right)_{el} = \left[(1-\beta)\rho_{M_{LS}} + \beta\rho_{M_{TB}}\right]g \qquad 3.40$$

$$\left(\frac{dP}{dL}\right)_{f} = \frac{2f_{F_{LS}}\rho_{M_{LS}}v_M^2}{ID}(1-\beta) \qquad 3.41$$

The acceleration component in the drillstring can be calculated by using Equations 3.33-3.35.

For fully developed Taylor bubble flow condition, β is given by

$$\beta = L_{TB} / L_{SU} \qquad 3.42$$

and $\rho_{M_{TB}} = \rho_G$

where $\rho_{M_{LS}}$ is calculated as in Equation 3.27 with changing H_L with $H_{L_{LS}}$, in addition the friction factor is calculated using the following mixture Reynolds number

$$N_{RE,M} = \frac{\rho_{M_{LS}} v_M ID}{\mu_L H_{L_{LS}} + \mu_G (1 - H_{L_{LS}})} \qquad 3.43$$

3.4.2 Upward Flow through the Annulus

- **Bubble Flow Model for Annular Geometries**

For a bubbly flow the holdup is calculated as reported by Hasan and Kabir[15] as follows :

$$H_L = 1 - \frac{v_{SG}}{v_\infty - C_O v_M} \qquad 3.44$$

C_O values are based on the inclination angle as shown in Table 3.1.

After calculating the holdup then mixture density and viscosity are calculated from Equations 3.27 and 3.28. The elevation pressure gradient is calculated using equation 3.29. For the frictional pressure loss is calculated from equation 2.30. Caetano[14,15] suggested the use of the calculation developed by Gunn and Darling[34] for a turbulent flow as follow

$$\left[f_F \left(\frac{F_P}{F_{CA}} \right)^{0.45 \exp\left[-(N_{RE}-3000)/10^6\right]} \right]^{-0.5} = 4 \log \left[N_{\mathrm{Re}} \left(f_F \left(\frac{F_P}{F_{CA}} \right)^{0.45 \exp\left[-(N_{RE}-3000)/10^6\right]} \right)^{0.5} \right] - 0.4 \qquad 3.45$$

where f_F is the Fanning friction factor.

Equation 3.45 has the following parameters:

F_P and F_{CA} are geometry parameters defined by the following equations

$$F_P = 16/N_{RE} \qquad 3.46$$

$$F_{CA} = \frac{16(1-K)^2}{\left[\frac{1-K^4}{1-K^2} - \frac{1-K^2}{\ln(1/K)} \right]} \qquad 3.47$$

K: diameter ratio is defined below

$$K = OD/ID \qquad 3.48$$

Where OD is the pipe outer diameter and ID is the inner casing diameter.

The mixture Reynolds number is calculated using Equation 3.31 the hydraulic diameter (D_h) used instead of the pipe inside diameter (ID).

The acceleration component is calculated using Beggs and Brill[5] approach using Equations 3.33-3.35

- **Dispersed Bubble Flow Model**

The dispersed bubble holdup is assumed equal to the no-slip holdup (λ_L). The same equations as in the bubble flow are used to calculate the total pressure gradient.

- **Slug Flow Model**

The same model used by Perez-Tellez[31] for the case of downward flow inside the drillstring is used. The hydraulic diameter is used instead of the inner tubing diameter in Equation 3.43 for calculating Reynolds number. In addition, the acceleration component can be calculated by

$$\left(\frac{dP}{dL}\right)_{acc} = \frac{H_{L_{LS}}\rho_L}{L_{SU}}\left(v_{L_{LS}} + \left|v_{L_{TB}}\right|\right)\left(v_{TB} - v_{L_{LS}}\right) \tag{3.49}$$

Finally the average holdup over the entire slug unit $H_{L_{SU}}$ for either developed of fully developing Taylor bubble can be calculated by[18]

$$H_{L_{SU}} = 1 - \frac{v_{SG} + \left(1 - H_{L_{LS}}\right)\left(v_{TB} - v_{G_{LS}}\right)}{v_{TB}} \tag{3.50}$$

- **Annular flow model**

Perez-Tellez[31] suggested using the model developed by Taitel and Barnea[35], where he stated that the use of this model will avoid convergence problems when implementing it into the computations.

Taitel and Barnea[35] stated that the total pressure drop in an annular flow can be calculated as follows :

$$\left(\frac{dP}{dL}\right)_{total} = \frac{r\tau_i}{D_e - 2\delta} + [\rho_L H_L + \rho_G(1-H_L)]g\ Sin\theta \qquad 3.51$$

The annular film thickness can be defined as follow

$$\delta = 0.115\left(\frac{\mu_L^2}{g(\rho_L - \rho_G)\rho_L}\right)^{1/3}\left(\frac{\rho_L v_{SL} D_e}{\mu_L}\right)^{0.6} \qquad 3.52$$

D_e is the equivalent pipe diameter and is calculated by

$$D_e = \sqrt{ID^2 - OD^2} \qquad 3.53$$

where ID is the inner casing diameter and OD is the outer pipe diameter.

The interfacial shear stress (τ_i) is defined by

$$\tau_i = \frac{0.5 f_i \rho_G v_{SG}^2}{\left[1 - 2(\delta / D_e)\right]^4} \qquad 3.54$$

The interfacial shear friction factor is calculated as suggested by Alves et al[35] as follows :

$$f_i = f_{sc} I \qquad 3.55$$

where f_{cs} is the superficial core friction factor (gas phase) and is calculated based on the core superficial velocity, density and viscosity. The interfacial correction parameter I is used to take into account the roughness of the interface. The parameter I is an average between the horizontal angle and the vertical angle and is calculated based on an inclination θ

$$I_\theta = I_H \cos^2\theta + I_V \sin^2\theta \qquad 3.56$$

The horizontal correction parameter is given by Henstock and Hanratty[36] :

$$I_H=1+800F_A \tag{3.57}$$

where

$$F_A = \frac{\left[(0.707N_{RE,SL}^2)^{2.5} + (0.0379N_{RE,SL}^{0.9})^{2.5}\right]^{0.4}}{N_{RE,SG}^{0.9}} \left(\frac{v_L}{v_G}\right)\left(\frac{\rho_L}{\rho_G}\right)^{0.5} \tag{3.58}$$

Where $N_{RE,SL}$ and $N_{RE,SG}$ are the superficial liquid and gas Reynolds number respectively. Both are calculated below

$$N_{RE,SL} = \frac{\rho_L v_{SL} ID}{\mu_L} \tag{3.59}$$

and

$$N_{RE,SG} = \frac{\rho_L v_{SG} ID}{\mu_G} \tag{3.60}$$

The vertical correction parameter is given by Wallis[37] as follow

$$I_V=1+300(\delta/D_e) \tag{3.61}$$

Finally considering a constant liquid film thickness, the liquid holdup can be calculated by

$$H_L = 4\left[\frac{\delta}{D_e} - \left(\frac{\delta}{D_e}\right)^2\right] \tag{3.62}$$

3.5 Bit Model

Perez-Tellez[31] developed a two phase bit model to handle the pressure drop across the bit nozzles. Using the mechanical energy balance[38] along with the gas weighting fraction and neglecting frictional pressure drop, he formulated the following expression for calculating the pressure drop across the bit nozzles :

$$\frac{v_n^2}{g_c}+\frac{(1-w_g)}{\rho_L}(P_{bh}-P_{up})+\frac{w_g zRT}{M_g}\ln\left(\frac{P_{bh}}{P_{up}}\right)=0 \qquad 3.63$$

where

v_n is the nozzle velocity

w_g is the gas weighing factor

P_{bh} is the bottomhole pressure

P_{up} is the upstream pressure

M_g is the gas molecular weight

Also using the continuity equation for the gas liquid mixture the following expression is reached to express the conservation of mass

$$\rho_M v_M A_n = q_L\rho_L + q_G\rho_G = \text{constant} \qquad 3.64$$

And the nozzle velocity is calculated by

$$v_n = \frac{q_G\rho_G + q_L\rho_L}{A_n}v \qquad 3.65$$

The above three equations are solved numerically to obtain the bit nozzle upstream pressure given the bottomhole pressure.

3.6 Fluid Properties

Several fluid properties need to be calculated when carrying the analysis either in the drillstring or the annulus. Several authors have published correlations for calculating such properties. Appendix A shows the calculations used to compute such properties.

Chapter 4

Computer Model

In Chapter 3, it was discussed how to utilize the mechanistic steady state model in order to model the flow behavior of an inclined well during UBD operation. In this work, the computer algorithm that was developed by Perez-Tellez[31] was modified and adjusted to handle a deviated wellbore. Specifically it was used to find a solution for the bottomhole pressure using the mechanistic models discussed previously.

The algorithm was coded into a macro which can be run using MS EXCEL®. The macro was written in VBA® (Visual Basic for Applications). Creating the code in EXCEL makes it easy to continue the analysis further into the same application or link it with other applications.

An incremental procedure for calculating the wellbore pressure traverse is used by the program. Increments of depth ΔL_i with an inclination angle θ_i from the horizontal. Figure 4.1 shows typical incremental calculations diagram in a deviated wellbore when carrying such type of pressure traverse calculations. As shows Figure 4.1, the calculations start at the annulus with a known starting pressure point (choke, surface) and then the calculations continue through the annulus taking into account different wellbore inclinations and different casing and drill pipe geometries. Inclination angles are read from the survey file and then a simple linear interpolation is used to find the angle at any depth. When the calculations reach the bottomhole, pressure drop through the bit nozzles is calculated. Next, calculations for downward flow in the drillstring are performed. Figure 4.2 shows a flow chart of the computer code used to carry out the pressure traverse calculations. For each length increment the inclination angle is calculated from the survey file provided or it can be input manually per the request of the user. The calculations for both the downward flow in the drillstring and upward flow in the annulus, and flow through bit

nozzles are performed using the models discussed in Chapter 3. Finally fluid properties are computed using the PVT correlations presented in Appendix A. Figure 4.2 shows the flowchart for modeling the calculations of the mechanistic steady state model in a deviated well while performing UBD operations.

In this model the user is required to input the following data through an EXCEL spreadsheet.

- Injection rates (gas and drilling fluid) at surface conditions (scf/min, and GPM)
- Surface temperature and pressure (surface or choke pressure), and the geothermal gradient.
- Survey data (measured depth, and inclination from horizontal).
- Drillstring and annular geometries. (OD, ID, hole size, pipe roughness).
- Depth at which calculations starts and either total depth or the depth at which the user wishes to finish calculations.
- Length increment.
- Drilling fluid properties (plastic viscosity and density).
- Bit nozzle diameters.
- Formation fluid production rates (bbl/day).

4.1 Field Example

The computer program described above has been used to simulate the behavior of a deviated well while drilling underbalanced using joint pipes with injection from the drillstring. In order to demonstrate the validity of the model, a field case was simulated and results compared with measurements. The field case is a previously drilled and cased well with a horizontal

sidetrack. Due to past history of lost circulation and the nature of the field there the decision was made to drill the well using UBD technique. Figure 4.3 shows the well suspension diagram.

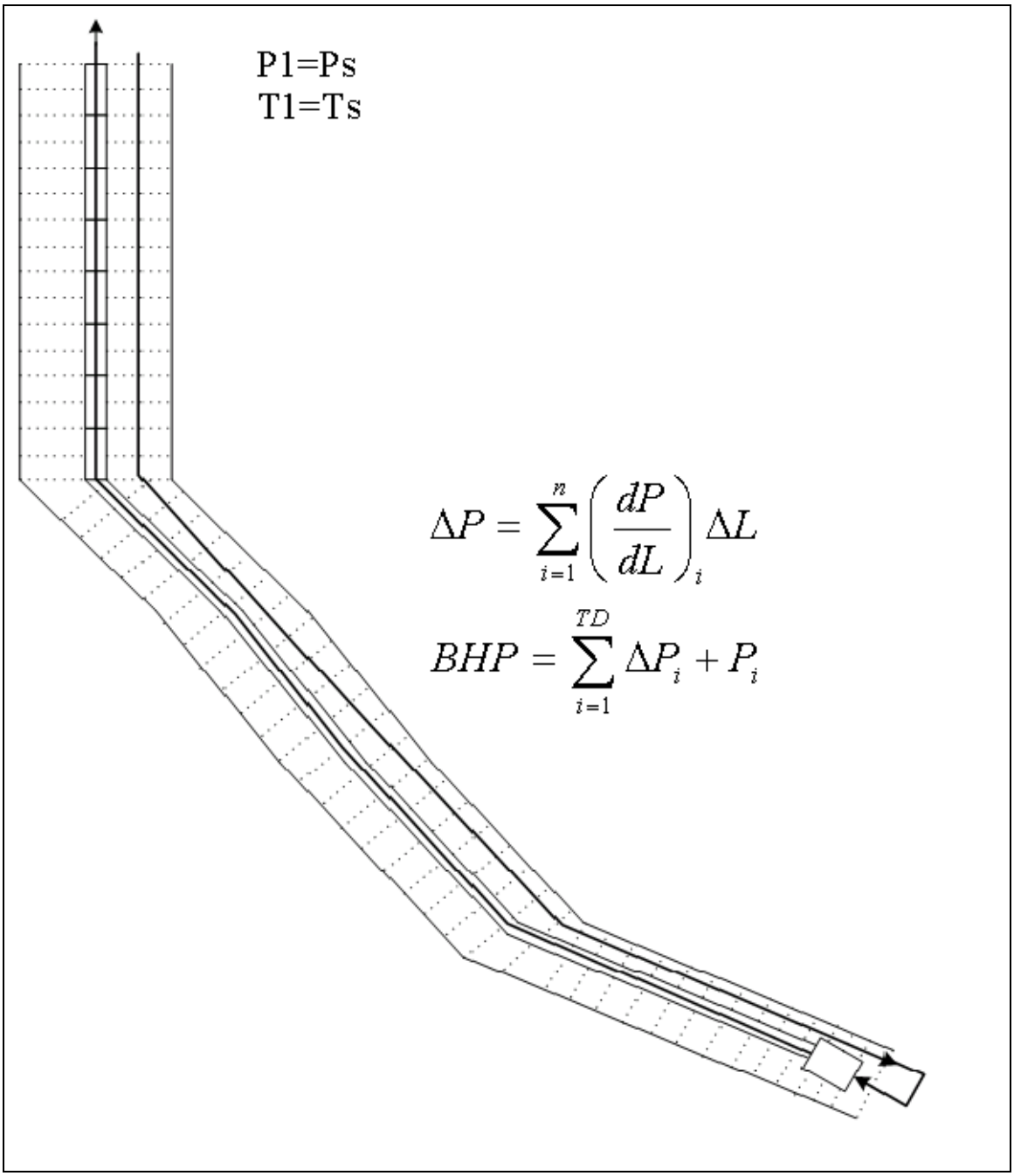

Figure 4.1: Incremental Wellbore Calculations Path in a Deviated Wellbore

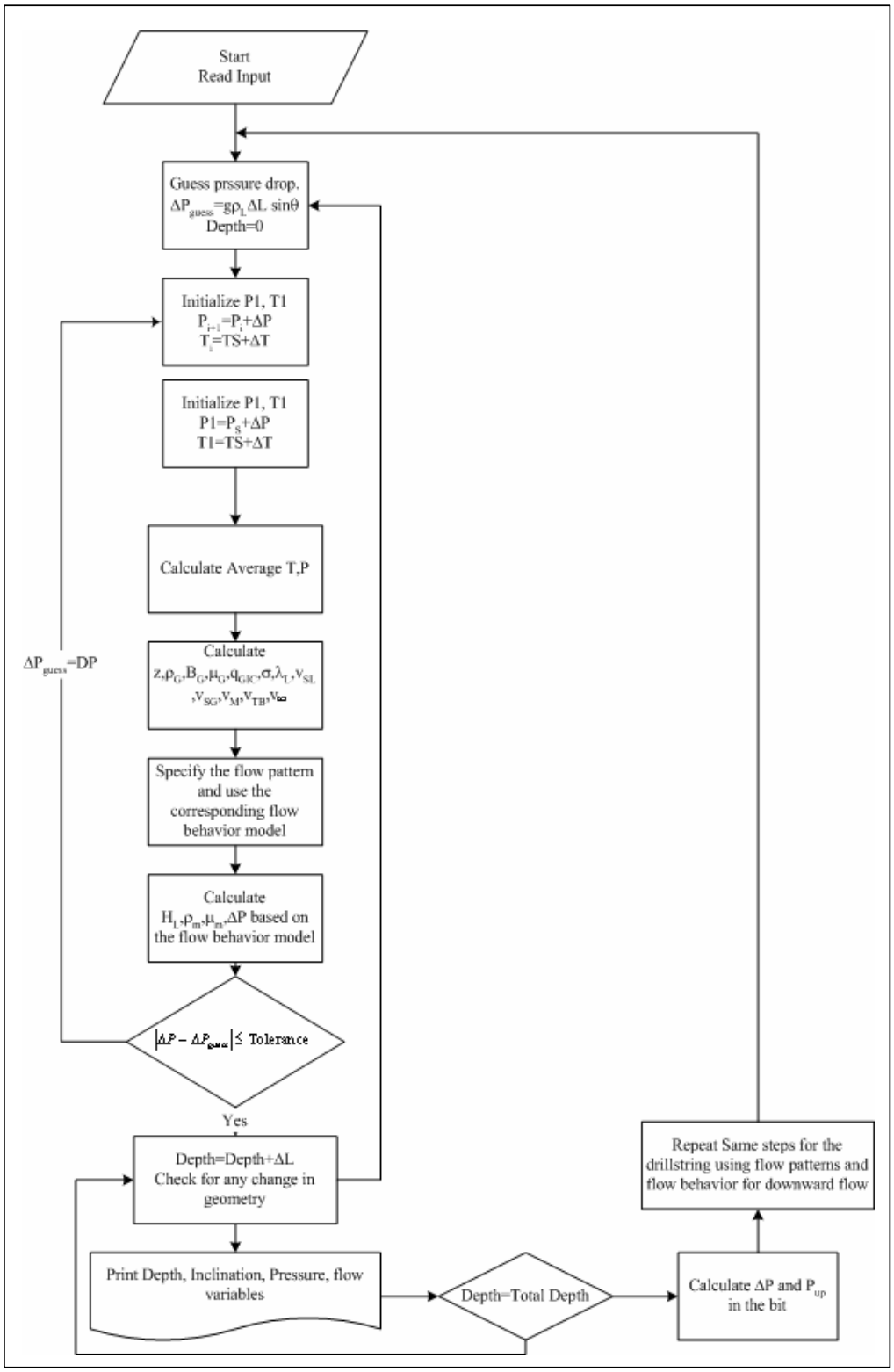

Figure 4.2 Flowchart for the Computer Algorithm Used in the Mechanistic Steady State Model

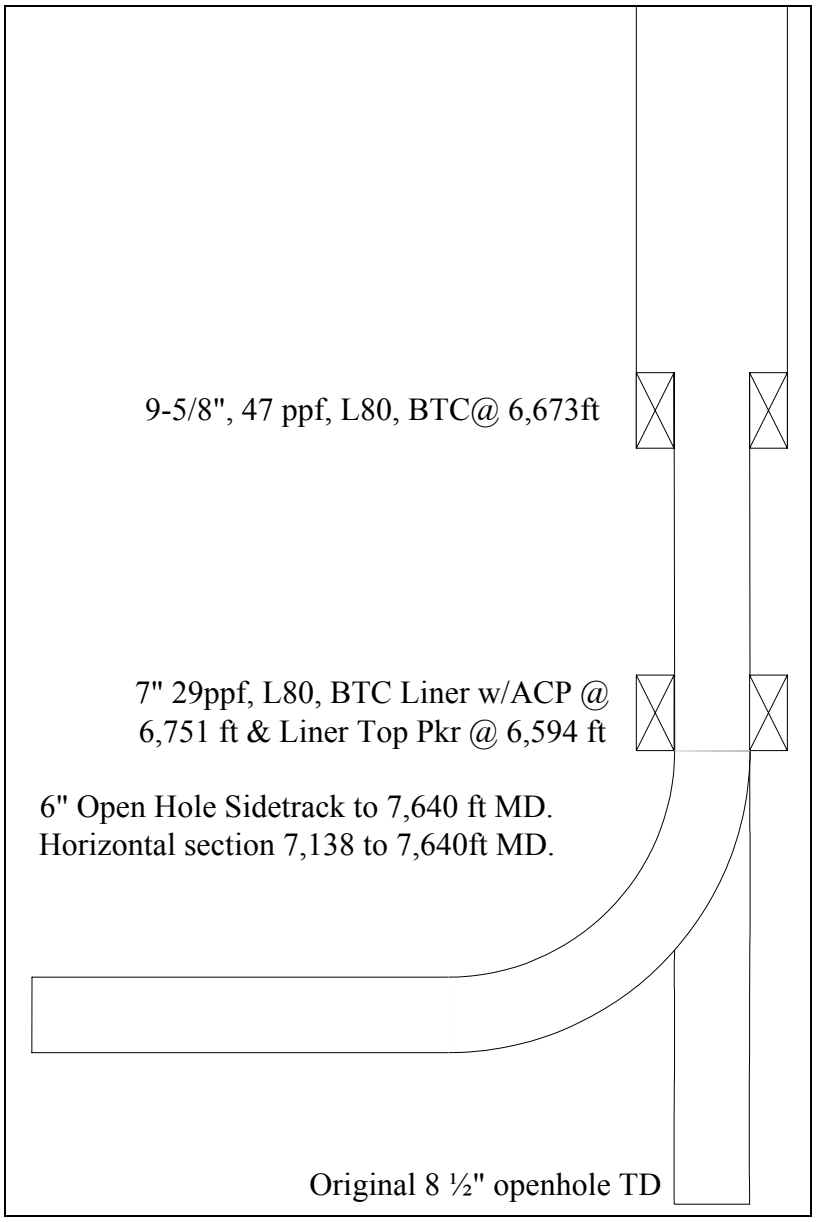

Figure 4.3: Well Suspension Diagram

As shown in Figure 4.3 the well is a re-entry well that was originally cased with 9-5/8" casing. A 7" velocity string was run to a depth 6,751 ft MD. Below the velocity string is a highly deviated 6" open hole sidetrack. The kick off point was at 6,742 ft MD and the well start landing at a depth of 7,138 ft MD where a horizontal section of about 502 ft was drilled. Figure 4.4 shows the survey plot of the well where the true vertical depth is plotted against the horizontal departure.

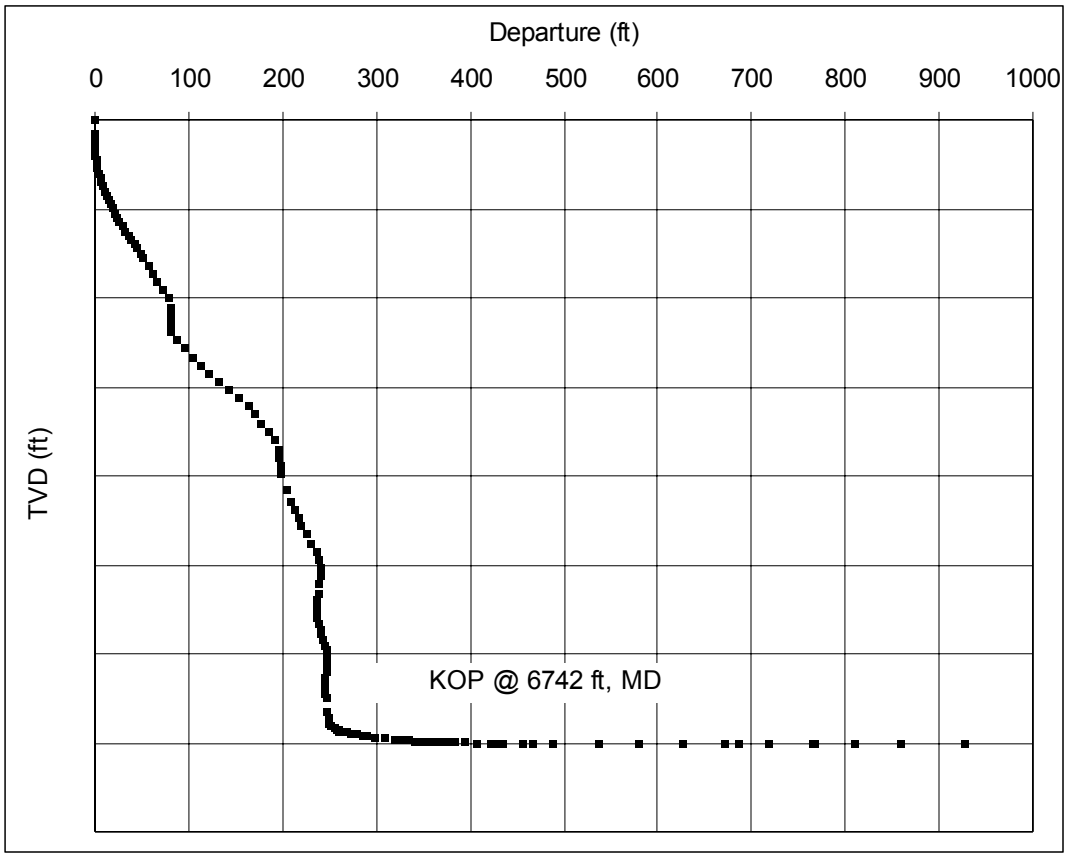

Figure 4.4 Survey Plot of True Vertical Depth vs. Horizontal Departure

During drilling, a pressure recording tool was installed above the bit to measure the bottomhole pressure (BHP). Simulation was carried out at two pressure points. The first one was at depth 7573 ft MD were they rotate drilling by pumping diesel at 270 gpm and N_2 at 670 scf/min with an injection pressure of 1700 psi. During that time the bottomhole pressure tool recorded a value of 2490 psi. The well produced oil at a rate of about 2520 bbl/day under these conditions. The second point was measured when reached the total depth 7640 ft MD, at this point, the diesel rate was 225 gpm and the N_2 rate was 1030 scf/min with an injection pressure of 1300 psi. Under these conditions the observed BHP was 2432 psi.

Table 4.1 shows annular and drillstring geometries for the above two depths. And Table 4.2 shows the input given to the EXCEL VBA program. The calculation incremental length

selected was taken for each 10 ft due to the sensitivity of the flow on the inclination angle. The horizontal section considered as a highly deviated section.

Table 4.1 : Drillstring and Annular Geometries at the Two Simulated Depths

Run #1					Run #2				
Annulus			Drillstring		Annulus			Drillstring	
Depth	Casing	Pipe OD	Depth	Pipe ID	Depth	Casing	Pipe OD	Depth	Pipe ID
ft	in	in	ft	in	ft	in	in	ft	in
0-6594	9.625	3.5	0-4528	2.6875	0-6594	9.625	3.5	0-4604	2.6875
6594-6751	7	3.5	4528-5078	2.1875	6594-6751	7	3.5	4604-5154	2.1875
6751-7547	6	3.5	5078-7478	2.4375	6751-7614	6	3.5	5154-7554	2.4375
Pressure tool to bit 26 ft			7478-7547	2.25	Pressure tool to bit 26 ft			7554-7614	2.25

Table 4.2 : Computer Program Input

Input	Run #1	Run #2	
Depth	7573	7640	ft
Gas flow rate at S. C.:	670	1030	scf/min
Liquid flow rate:	270	225	gpm
Liquid density:	7.910	7.910	ppg
Mud viscosity	3.00	3.00	cp
Length increment (DL):	10.00	10.00	ft
Bit Nozzle size (3 nozzles):	16.00	18.00	(1/32) in
Reservoir Influx	2520	6000	bbl/day

After running the program for the two cases, the results have a good match with the measured value where at the average absolute error E_a has an average value of less than 10% (about 87 psi) as shown in Table 4.3. Equation 4.1 gives the expression for E_a.

$$E_a = \left| \frac{P_{calc} - P_{meas.}}{P_{meas}} \right| x100 \qquad 4.1$$

A commercial simulator was used to compare the results of this study to the simulator output; this recent version of the simulator uses the empirical correlation that was developed by Hasan and Kabir. Table 4.3 shows the output result of the developed model in this study with the result of the simulator output.

Table 4.3 : Comparison of Absolute Average Error for the Two Simulation Runs

Comparison		Run #1		Run #2	
		Calc	Ea	Calc	Ea
Developed Model	BHP	2585	3.797	2494	2.564
	P_{inj}	1882	10.690	1198	7.860
Simulator-Beggs & Brill	BHP	2366	4.980	2282	6.160
	P_{inj}	2040	20.012	1614	24.185
Simulator-Hasan & Kabir	BHP	2694	8.177	2622	7.792
	P_{inj}	1675	1.476	1371	5.485

Table 4.3 shows that the developed model has a very good agreement with the observed data for both depths as shown from the absolute relative error values. The used commercial simulator is based on empirical correlations; the simulator was run using the well known Beggs-Brill and Hasan-Kabir correlations (most recent as specified by the simulator manufacturer). The results shown in Table 4.3 indicate that the simulator predict the bottomhole pressure reasonably well however the mechanistic model outperform runs both. Also as shown in Table 4.7, despite the fact that the recent correlation by Hasan-Kabir works well for the first run it didn't calculate the correct bottomhole pressure for the second run. For the second run the pressure difference between the calculated and the measured pressure was about 190 psi, compared to a difference of only 50 psi in the modified developed model in this study. Also, the modified developed mechanistic steady state model shows a consistency of pressure distribution along the drill pipe and annulus for both runs, despite the fact that is appear to be Beggs and Brill correlation works well for the run at 7640 ft MD but the correlation didn't model correctly the distribution along

the wellbore and gave a large injection pressure. In addition, the use of different mechanistic models shows that they can capture the behavior of the flow during different combination of flow rates and pipe geometries, unlike the empirical correlations where they reported not to work well in oil field cases, and also they were developed by production engineers to handle either upward flow during the pipe or the annulus. Another reason why such large error occurred is the fact that this well has a large horizontal section which is this case was treated as highly deviated; hence the calculations may be affected by this assumption.

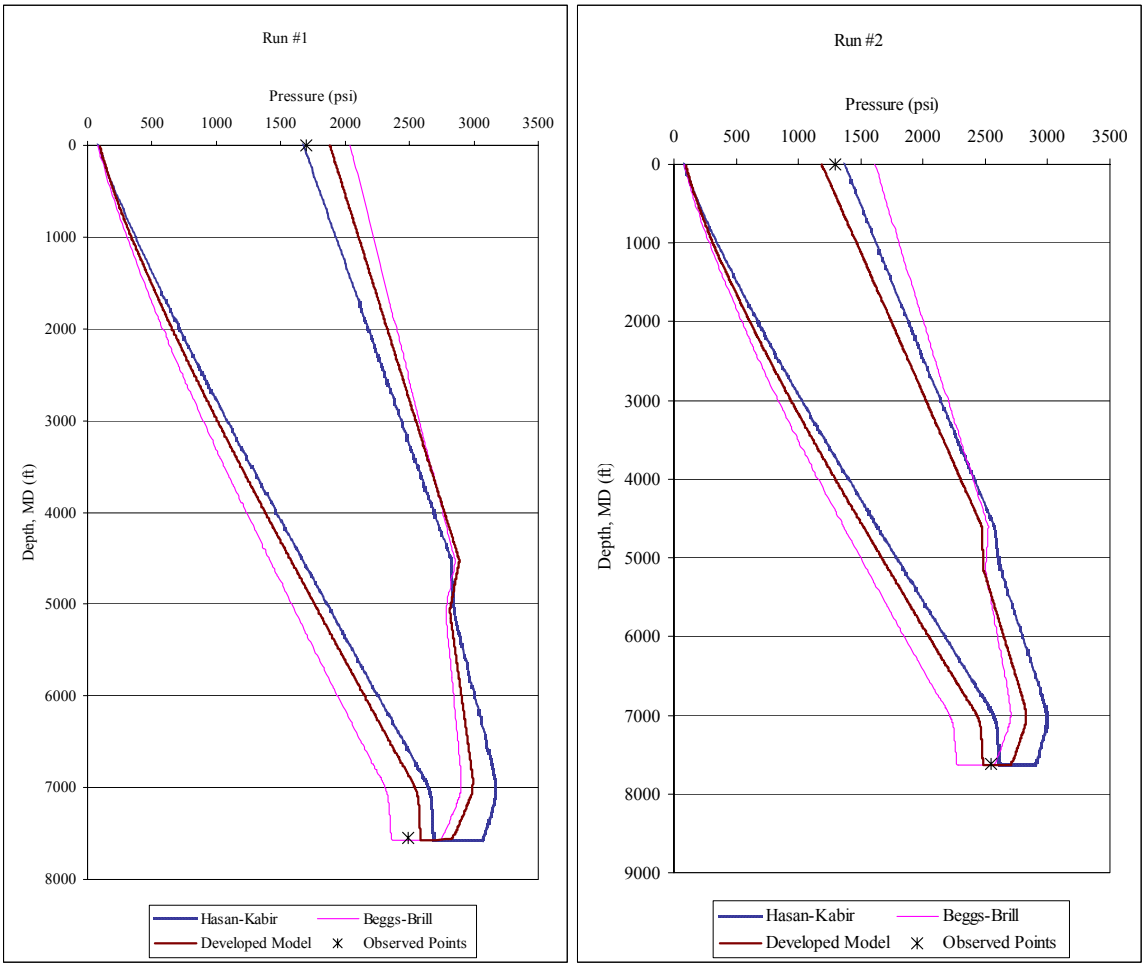

Figure 4.5: Comparison between Field Measurements and Simulators Output at Both Runs

Figure 4.5 shows a plot of the two simulators results with the measured data for both simulated depths. The effect of inclination is seen thoroughly in the developed model whereas the commercial simulator shows changes in the geometry where it will effect the flow behavior. Also the combination use of mechanistic steady state models has eliminated any sharp transition in the calculations, which is not the same case for commercial simulator output.

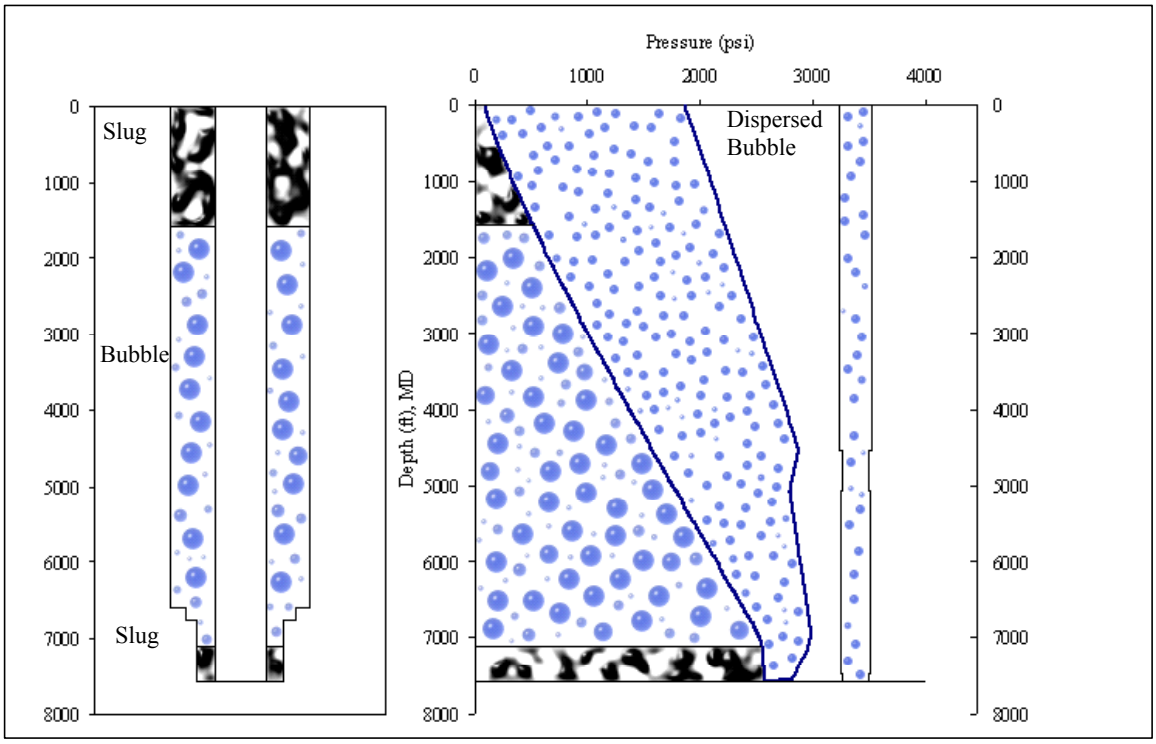

Figure 4.6 : Composite Plot of Pressure Distribution along with Well Geometry for Run #1

Figure 4.6 above shows a composite plot of the pressure distribution along the annulus and the drill pipe. As shown during injection the flow pattern in the drill pipe is dispersed bubble due to the high liquid velocity and low gas velocity in which it exists when using N_2 to lighten the drilling fluid. In the annulus and in the horizontal section, slug flow exists to a depth of 7,101 ft MD, due to the large liquid slugs exists and pressure drops across bit nozzles cause such affect. Bubble flow exists from 7,101 ft MD to a depth of 1590 ft MD where slug flow exists from 1590 ft MD to the surface in the annulus.

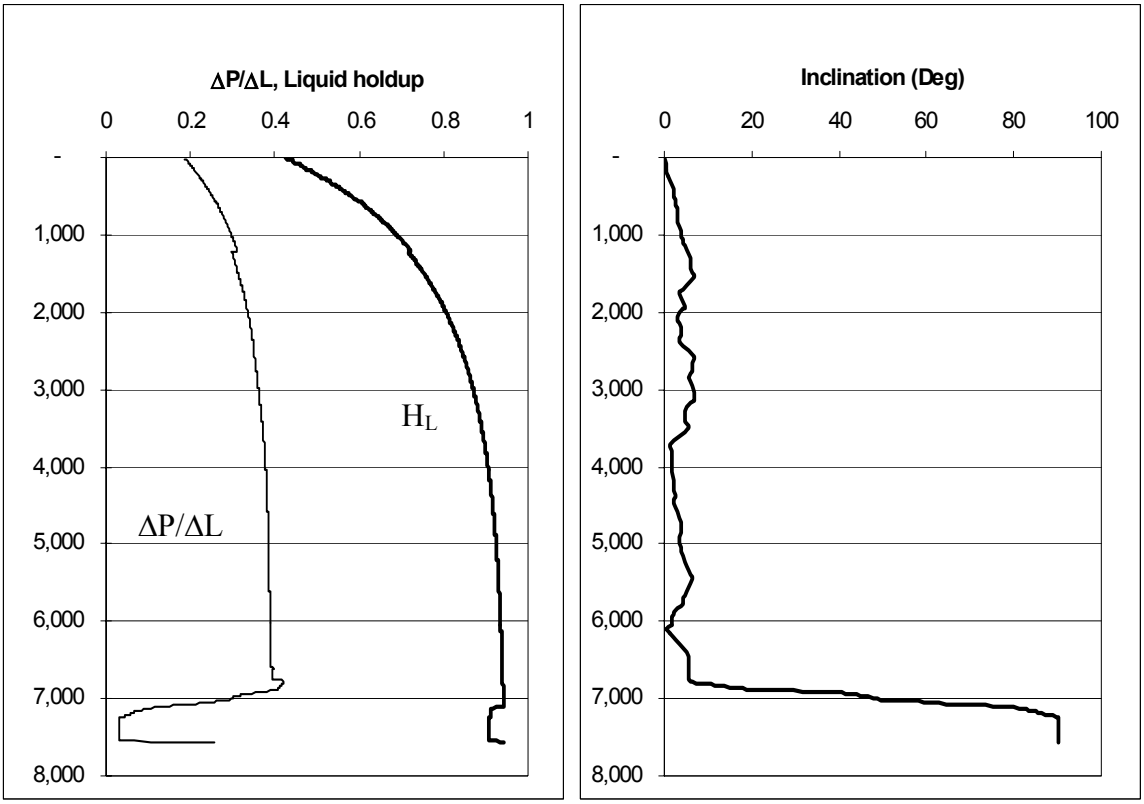

Figure 4.7: Simulation Results (H_L, $\Delta P/\Delta L$) vs Depth at Run #1 in the Annulus

Figure 4.7 shows a plot of the pressure gradient, liquid holdup and inclination angle against measured depth. It can be seen that both the pressure gradient and liquid holdup changes with the start of the horizontal section where the pressure gradient decreased (expected in nearly horizontal flow) due to the decrease in the elevation component in the total pressure gradient computations where it has the effect shown in the figure above.

Chapter 5

Conclusion and Recommendations

5.1 Conclusions

- The use of mechanistic steady state model has proven to give better prediction than empirical correlations especially when trying to design UBD operation within a pressure window.
- The developed model and the computer program is only valid to steady-state conditions.
- The combination of flow prediction and flow behavior models has proven to effectively predict flow profile in a steady state condition.
- The development of the computer program in EXCEL VBA® will ease both its use and further development.
- The program can be used in spreadsheet calculations to carry several models and predictions.
- The use of the marching algorithm is recommended taking into account selection of the appropriate length increment since if the survey data was taken alone this will have an increase effect on the calculations. Also a simple interpolation is used in order to find the inclination angle from the horizontal at each given depth.
- The bit model used has proven to work in estimating injection pipe pressure as shown between the comparison between the results of the simulator and the developed model in this study.

- This program can be used also to calculate the pressure drop in conditions other and than UBD operations. However, some modifications are needed in order to accommodate for variables fluid influx from the reservoir.
- This tool can be used as a design tool where UBD controlled surface parameters such as injection rates and choke pressures are calculated in order to drill the reservoir within the desired UBD window required by the first design of the UBD operation.
- It is shown in the field example calculations that the assumptions of highly deviated wells have affected the calculations but not as large as when using the correlations.

5.2 Recommendations

- Any future development of mechanistic models should improve results by increasing accuracy in liquid holdup and pressure gradient predictions.
- Developing a model for a truly horizontal increment are recommended also to enhance the calculations and create a unified model for all angle ranges.
- The developed model can be coupled with the time dependent model developed by Perez-Tellez[31] and find an un-steady state solution for deviated wellbores drilled under UBD conditions. This will allow analysis of the well during pipe connections.

REFERENCES

1 Gas Research Institute (GRI), Underbalanced Drilling Manual, published by Gas Research Institute, Chicago, Illinois, 1997.

2 Bennion D.B and Thomas F.B.: "Underbalanced Drilling of Horizontal Wells: Does It Really Eliminate Formation Damage?" paper 27352 presented at the SPE Intl. Symposium on Formation Damage Control held in Lafayette, Louisiana, February 7-10, 1994.

3 Guo, B, Hareland G., and Rajtar, J.: "Computer Simulation Predicts Unfavorable Mud Rate for Aerated Mud Drilling", paper SPE 26892 presented at the 1993 SPE Eastern Regional Conferences held in Pittsburgh, Pa. Nov. 2-4 1993.

4 Liu, G. and Medley, G.H.: "Foam Computer Model Helps in Analysis of Underbalanced Drilling", *Oil and Gas J.* July 1,1996.

5 Beggs, H.D. and Brill, J.P.: "A Study of Two phase Flow in Inclined Pipes", JPT. May 1973. pp. 607-617.

6 Maurer Engineering Inc.: Underbalanced Drilling and Completion Manual, copyrighted 1998, DEA-101, Houston, Texas.

7 Maurer Engineering Inc.: Air/Mist/Foam/ Hydraulics Model, User's Manual, copyrighted 1998, DEA-101, Houston, Texas.

8 Tian, S., Medley G.H. Jr., and Stone, C.R.: "Optimizing Circulation While Drilling Underbalanced", *World Oil*, June 2000, pp 48-55.

9 Tian, S., Medley G.H. Jr.: "Re-evaluating Hole Cleaning in Underbalanced Drilling Applications", paper presented at the IADC Underbalanced Drilling Conference and Exhibitions, Houston, Texas, August 28-29 2000.

10 Bijleveld, A.F., Koper, M., and Saponja, J.: "Development and Application of an Underbalanced Drilling Simulator", paper IADC/SPE 39303 presented at the 1996 IADC/SPE Drilling Conferences held in Dallas, Texas, March 3-6, 1996.

11 Ansari, A.M., Sylvester, N.D., Sarica, C., Shoham, O., and Brill, J.P.: "A Comprehensive Mechanistic Model for Upward Two Phase Flow in Well bores," SPE Production and Facil., p. 143, May (1994).

12 Gomez, L., Shoham, O., Schmidt, Z., Chokshi, R., Brown, A., and Northug, T.: "A Unified Mechanistic Model for Steady-State Two phase Flow in Wellbores and Pipelines," paper SPE 56520 presented at the 1999 ATCE Houston, Texas, October 3-6, 1999.

13 Kaya, A.S., Sarica, C., and Brill, J.P.: "Comprehensive Mechanistic Modeling of Two phase Flow in Deviated Wells," paper SPE 56522 presented at the 1999 Annual and Technical Conferences and Exhibition, Houston, TX, October 3-6, 1999.

14 Caetano, E.F., Shoham, O., and Brill, J.P.: "Upward Vertical Two phase Flow Through Annulus Part I: Single-Phase Friction Factor, Taylor Bubble Rise Velocity, and Flow Pattern Prediction," *Journal of Energy Resources Technology* (1992) 114, 1.

15 Caetano, E.F., Shoham, O., and Brill, J.P.: "Upward Vertical Two phase Flow Through Annulus Part II: Modeling Bubble, Slug, and Annular Flow," *Journal of Energy Resources Technology* (1992) 114, 14.

16 Hasan, A.R. and Kabir, C.S: "Tow-Phase Flow in Vertical and Inclined Annuli," *Intl. J. Multiphase Flow* (1992) 18, 279.

17 Lage, A.C.V.M and Timer.: "Mechanistic Model for Upward Tow-Phase Flow in Annuli," paper 63127, presented at the 2000 SPE ATCE help in Dallas, Texas, October 1-4, 2000.

18 Perez-Téllez, C., Smith, J.R., and Edwards, J.K.: "A New Comprehensive, Mechanistic Model for Underbalanced Drilling Improves Wellbore Pressure Predictions", paper SPE 74426 presented at the 2002 IPCEM held in Villahermosa, Mexico, February 10-12, 2002.

19 Gavignet, A.A., and Sobey, I.J.: "A Model for The Transport of Cuttings in Highly Deviated Wells," paper 15417, presented at the 1986 SPE ATCE held in New Orleans, Louisiana, October 5-8, 1986.

20 Brown, N.P., Bern, P.A., and Weaver, A.: "Cleaning Deviated Holes: New Experimental and Theoretical Studies," paper 18636, presented at the 1986 SPE/IADC conference held in New Orleans, Louisiana, February.

21 Brill, J.P. and Mukherjee, H.: Multiphase Flow in Wells, Monograph Volume 17 copyright 1999 by the Society of Petroleum Engineers Inc.

22 Beggs, H.D.: Production Optimization Using Nodal Analysis, OGCI publications, Oil and Gas Consultants International Inc. Tulsa, OK, 1991.

23 Taitel, Y., Barnea, D. and Duckler, A.E.: "Modeling Flow Pattern Transitions for Steady Upward Gas-Liquid Flow in Vertical Tubes", *AIChE J.* (1980) 26, pp 345-354.

24 Hasan, A.R.: "Void Fraction in Bubbly and Slug Flow in Downward Vertical and Inclined Systems", paper SPE 26522, presented at 1993 Annual Technical Conference and Exhibition held in Houston, TX, October 3-6, 1993.

25 Hasan, A.R.: “Inclined Two phase Flow: Flow Pattern, Void Fraction and Pressure Drop in Bubbly, Slug and Churn Flow,” *Particulate Phenomena and Multiphase Transport*, Hemisphere Publishing Corp., New York city (1988), 229.

26 Hasan, A.R. and Kabir, C.S.: “Predicting Multiphase Flow Behavior in a Deviated Well,” SPEDE (Nov, 1988), 474.

27 Harmathy, T.Z.: “Velocity of Large Drops and Bubbles in Media of Infinite or Restricted Extent,” *AIChE J.* (1960) 6, 281-288.

28 Zuber, N. and Findlay, J.A.: “Average Volumetric Concentration in Two Phase Flow System”, Journal of Heat Transfer, pages 453-468, November 1965.

29 Alves, I. N.: Slug Flow Phenomena in Inclined Pipes, Ph.D. Dissertation, The University of Tulsa, Tulsa, Oklahoma, 1991.

30 Wallis, G.B.: One Dimensional Two phase Flow, McGraw-Hill (1969).

31 Perez-Tellez, C.: Improved Bottomhole Pressure Control for Underbalanced Drilling Operations, Ph.D Dissertation, Louisiana State University (2002).

32 Tengesdal, J.O., Kaya, A.S., and Cem Sarica.: “Flow Pattern Transition and Hydrodynamic Modeling of Churn Flow,” *SPE J* (December 1999) 4, No. 4, pp 342-348.

33 Colebrook, C.F.: “Turbulent Flow in Pipes With Particular Reference to the Transition Region Between the Smooth and Rough Pipe Laws,” *J. Inst. Civil Eng.* (1939), 11, 133.

34 Gunn, D.J. and Darling, C.W.W.: “Fluid Flow and Energy Losses in Non Circular Conduits,” Trans. AIChE (1963) 41, 163.

35 Taitel, Y. nd Barnea, D.: “Counter Current Gas-Liquid Vertical Flow, Model for Flow Pattern and Pressure Drop,” *Int. J. Multiphase Flow* (1983) 9, 637-647.

36 Alves, I. N., Caetano, E. F., Minami, K. and Shoham, O.: "Modeling Annular Flow Behavior for Gas Wells," SPE Production Engineering, (November 1991), 435-440

37 Henstock, W.H. and Hanratty, T.J.: “The Interfacial Drag and the Height of the Wall Layer in Annular Flow”, *AIChE J.*, 22, No. 6, (Nov. 1976),990-1000.

38 Wallis, G.B.: One Dimensional Two phase Flow, McGraw-Hill (1969).

39 Bourgoyne, A.T. Jr., Chenevert M.E., Millheim, K.K., and Young, F.S.: Applied Drilling Engineering, SPE textbook series, 1984.

40 Dranchuk, P.M., and Abu-Kassem, J.H.: “Calculations of Z-Factors for Natural Gases Using Equation of State,” *J. Canadian Pet. Tech.* (July-Sep 1975)14, 34

41 Standing, M.B., and Katz, D.L.: “Density of Natural Gases,” *Trans.* ,AIME (1942) 146, 140

42 Lee, A.L., et al.: “The Viscosity of Natural Gases,” *JPT*, Aug., 1966.

43 Beggs, H. D. and Robinson, J. R.: “Estimating the Viscosity of Crude Oil Systems,” *JPT*, Sept, 1959.

Appendix A: PVT Correlations

The following correlations are implemented into the computer algorithm in order to calculate fluid properties at different pressures and temperatures.

Gas Compressibility Factor

Dranchak and Abu-Kassem[39] correlate the Standing and Katz[40] Z-Factor diagram where they reached to the following solution in which it can be solved by a trial and error procedure.

$$z = \left(A_1 + \frac{A_2}{T_{pr}} + \frac{A_3}{T_{pr}^3} + \frac{A_4}{T_{pr}^4} + \frac{A_5}{T_{pr}^5} \right) \rho_r + \left(A_6 + \frac{A_7}{T_{pr}} + \frac{A_8}{T_{pr}^2} \right) \rho_r^2 - A_9 \left(\frac{A_7}{T_{pr}} + + \frac{A_8}{T_{pr}^2} \right) \rho_r^5 + A_{10} \left(1 + A_{11} \rho_r^2 \right) \frac{\rho_r^2}{T_{pr}^3} \exp\left(- A_{11} \rho_r^2 \right) + 1.0 \quad \text{A.1}$$

$$\rho_r = \frac{0.27 P_{pr}}{z T_{pr}} \quad \text{A.2}$$

A_1 to A_{11} are constant and shows in the table below

Table A.1 Constants Used in Dranchak and Abu-Kassem[38] Correlation

$A_1 = 0.3265$	$A_4 = 0.01569$	$A_7 = -0.7361$	$A_{10} = 0.6134$
$A_2 = -1.0700$	$A_5 = -0.05165$	$A_8 = 0.1844$	$A_{11} = 0.7210$
$A_3 = -0.5339$	$A_6 = 0.5475$	$A_9 = 0.1056$	

Gas Viscosity

Lee et al.[41] developed the following equations for calculating gas viscosities at in-situ temperature as follows :

$$\mu_G = A x 10^4 \exp\left(1000 B \rho_G^C\right) \quad \text{A.3}$$

$$A = \frac{(9.4 + 0.02M_G)T^{1.5}}{209} + 19M_G + T \quad \text{A.4}$$

$$B = 3.5 + 0.01M_G + \frac{986}{T} \quad \text{A.5}$$

$$C = 2.4 - 0.2B \quad \text{A.6}$$

Gas Surface Tension

The following equations were used to compute the gas surface tension[21] at any temperature where $\overline{T}$ is average temperature between surface and any given depth.

$$\sigma_{w(74)} = 75 - 1.108P^{0.349} \quad \text{A.7}$$

$$\sigma_{w(280)} = 53 - 0.1048P^{0.637} \quad \text{A.8}$$

$$\sigma_G = \frac{\sigma_{74} - (\sigma_{74} - \sigma_{280})\left(\frac{\overline{T} - T_{surf}}{T - T_{surf}}\right)}{1000} \quad \text{A.9}$$

Oil Viscosity

Oil viscosity is calculated using Beggs and Robinson[42] equations as follows:

$$\mu_{oil} = A_{oil}(10^x - 1.0)^{B_{oil}} \quad \text{A.10}$$

$$x = YT^{-1.163} \quad \text{A.11}$$

$$Y = 10^{3.0324 - 0.0203(API)} \quad \text{A.12}$$

$$A_{oil} = 10.715x(150)^{-0.515} \quad \text{A.13}$$

$$B_{oil} = 5.44x(150)^{-0.338} \quad \text{A.14}$$

Appendix B: NOMENCLATURE

$(dP/dL)_{acc}$	Acceleration pressure gradient, (psi/ft)
$(dP/dL)_{el}$	Elevation pressure gradient, (psi/ft)
$(dP/dL)_{f}$	Frictional pressure gradient, (psi/ft)
$(dP/dL)_{total}$	Total pressure gradient, (psi/ft)
A_L	Liquid area in pipe element (m^2,in^2)
A_n	Bit nozzle area (m^2,in^2)
A_P	Pipe element area, (m^2,in^2)
C_1	Velocity profile coefficient for slug flow
C_O	Velocity profile coefficient for bubbly flow
D_e	Equivalent pipe diameter, (m/in)
D_{ep}	Equi-periphery diameter, (m/in)
D_h	Hydraulic diameter, (m/in)
Ea	absolute average relative error
f_F	Fanning friction factor
f_i	Interfacial shear friction factor for annular flow
f_M	Mixture friction factor
F_P,F_{CA},K	Geometry parameters in calculating fanning friction factor for bubbly flow
f_{SC}	Superficial core friction factor
H_L	Liquid holdup
H_L^n	Liquid holdup with swarm effect
$H_{L_{LS}}$	Liquid Holdup in liquid slug zone
$H_{L_{SU}}$	Liquid Holdup in a slug unit
$H_{L_{TB}}$	Liquid Holdup in Taylor bubble in a slug flow
ID	Inner diameter (m,in)
$L_{L_{LS}}$	Liquid length in liquid slug zone
$L_{L_{TB}}$	Length of slug unit
$L_{L_{TB}}$	Slug length in Taylor bubble in a slug
M_g	Gas molecular weight
N_{RE}	Reynolds Number
$N_{RE,M}$	Mixture Reynolds number
$N_{RE,SG}$	Superficial gas Reynolds number

$N_{RE,SL}$	Superficial liquid Reynolds number
OD	Outer diameter (m,in)
P_{bh}	Bottom hole pressure (Pa,psi)
P_{calc}	Calculated Pressure (Pa,psi)
P_{meas}	Measured Pressure (Pa,psi)
P_{up}	Upstream pessure (Pa,psi)
q_G	Gas flow rate (scf/m)
q_L	Liquid flow rate, (m^3/s, gpm)
R	Universal Gas constant = 10.731 psia.ft^3/lbm.mol.°R
T	Temperature (°K,°R)
τ_i	Interfacial shear, (Pa,psi)
w_g	Gas weighing factor
Z	Gas compressibility factor
β	Relative bubble length parameter in a slug flow
δ	Liquid film thickness in flow model(m,ft)
λ_L	No slip liquid holdup
μ_G	Gas viscosity, (Pa.s, cp)
μ_L	Liquid viscosity, (Pa.s, cp)
μ_M	Mixture viscosity, (Pa.s, cp)
θ	Inclination angle from horizontal
ρ_G	Gas density, (kg/m^3,ppg)
ρ_L	Liquid density (kg/m^3,ppg)
ρ_M	Mixture density, (kg/m^3,ppg)
ρ_{ML}	Mixture density in liquid slug, (kg/m^3,ppg)
ρ_{MTB}	Mixture density in Taylor bubble in a slug, (kg/m^3,ppg)
v_∞	Discrete gas bubble rise velocity, (m/s,ft/s)
v_G	Gas velocity, (m/s,ft/s)
v_L	Liquid velocity, (m/s,ft/s)
$v_{L_{LS}}$	Liquid velocity in liquid slug zone, (m/s,ft/s)
$v_{L_{TB}}$	Taylor bubble velocity in a slug, (m/s,ft/s)
v_n	Nozzle velocity, (m/s,ft/s)
v_{SG}	Superficial gas velocity (m/s,ft/s)
v_{SL}	Superficial liquid velocity (m/s,ft/s)
v_{TB}	Taylor bubble rise velocity, (m/s,ft/s)

VITA

Faisal Abdullah ALAdwani Born in Kuwait city, Kuwait, in October 10, 1975. In January 1998, he received a degree Bachelor of Science in Petroleum Engineering from Kuwait University. In March 1998, he joined Kuwait Foreign Petroleum Exploration Company where he worked as a petroleum engineer and was assigned to field operations in the Southeast Asia Region. In August 2001, he joined the Craft & Hawkins Petroleum Engineering Department at Louisiana State University to work towards a Master of Science in Petroleum Engineering. He is a member of the Society of Petroleum Engineers.